

Modular Domain Structure: A Biomimetic Strategy for Advanced Polymeric Materials

Zhibin Guan,* Jason T. Roland, Jane Z. Bai, Sharon X. Ma, Theresa M. McIntire, and Maianh Nguyen

Contribution from the Department of Chemistry, 516 Rowland Hall, University of California, Irvine, California 92697-2025

Received October 20, 2003; E-mail: zguan@uci.edu

Abstract: A long lasting challenge in polymer science is to design polymers that combine desired mechanical properties such as tensile strength, fracture toughness, and elasticity into one structure. A novel biomimetic modular polymer design is reported here to address this challenge. Following the molecular mechanism used in nature, modular polymers containing multiple loops were constructed by using precise and strong hydrogen bonding units. Single-molecule force-extension experiments revealed the sequential unfolding of loops as a chain is stretched. The excellent correlation between the single-molecule and the bulk properties successfully demonstrates our biomimetic concept of using modular domain structure to achieve advanced polymer properties.

Introduction

Mechanical properties are among the most fundamental properties of polymeric materials.¹ Despite the great progress made in recent years in polymeric materials science and technologies,^{2,3} it remains a great challenge to design a polymer that combines important mechanical properties such as tensile strength, fracture toughness, and elasticity into one structure, because these properties usually require different molecular mechanisms and, hence, are generally considered exclusive to each other.⁴ Nature, on the other hand, has evolved complex and elegant polymeric materials that combine these properties fulfilling a myriad of functions. Nature achieves this by precisely controlling the molecular and nanoscopic structures of biomacromolecules such as proteins. The secondary and tertiary structures of proteins are not only important for their biological functions but also critical for their superior material properties. For example, silks,⁵ cell adhesion proteins,⁶ and connective proteins existing in both soft and hard tissues such as muscle,^{7–10} seashell,¹¹ and bone¹² exhibit a remarkable combination of high

strength, toughness, and sometimes elasticity as well, three properties that are rarely found in one synthetic polymer.⁴ Recent single-molecule nanomechanical studies revealed that the combination of these mechanical properties in natural materials arise from their unique molecular and nanoscopic structures.^{7–10} The biopolymers in these systems share a common modular structure composed of a linear array of nanodomains, in which each domain is held together by secondary interactions, e.g., hydrogen-bonding, hydrophobic, and van der Waals interactions. One marvelous example of this modular design is titin, a giant protein of muscle sarcomere that has 200–300 repeating modules (Figure 1). Sequential unfolding of the titin domains results in a saw-tooth pattern in the force–extension curve, with each peak corresponding to the unfolding of an individual domain.^{5–12} The saw-tooth shaped force–extension curves reflect a constant force sustained over the entire extension, which makes the polymer *strong*, along with a large area under the force–extension curve, making it *tough* as well.¹¹ In addition, when the external force is removed, the unfolded domains of modular proteins will refold automatically, making them *elastic*.

Here we report the first application of this elegant molecular mechanism commonly employed in nature to address a long-standing challenge in material science: to design polymers having precise molecular nanostructures that combine high strength, toughness, and elasticity. In contrast to natural polymers, synthetic polymeric materials usually lack precise higher ordered structures, despite the fact that significant progress has been made in designing short oligomers with well-defined secondary structures.^{13–20} Furthermore, there is a gap in connecting the single-molecule properties with the bulk

- (1) Hearle, J. W. S. *Polymers and Their Properties, Vol. 1: Fundamentals of Structure and Mechanics*; 1982.
- (2) Krejchi, M. T.; Atkins, E. D. T.; Waddon, A. J.; Fournier, M. J.; Mason, T. L.; Tirrell, D. A. *Science* **1994**, *265*, 1427–1432.
- (3) Rathore, O.; Sogah, D. Y. *J. Am. Chem. Soc.* **2001**, *123*, 5231–5239.
- (4) Booth, C., Price, C., Eds. *Comprehensive Polymer Science: The Synthesis, Characterization, Reactions, and Applications of Polymers, Vol. 2: Polymer Properties*; 1989.
- (5) Oroudjev, E.; Soares, J.; Arcidiacono, S.; Thompson, J. B.; Fossey, S. A.; Hansma, H. G. *Proc. Natl. Acad. Sci. U.S.A.* **2002**, *99*, 6460–6465.
- (6) Law, R.; Carl, P.; Harper, S.; Dalhaimer, P.; Speicher, D. W.; Discher, D. E. *Biophys. J.* **2003**, *84*, 533–544.
- (7) Rief, M.; Gautel, M.; Oesterhelt, F.; Fernandez, J. M.; Gaub, H. E. *Science* **1997**, *276*, 1109–1112.
- (8) Kellermayer, M. S. Z.; Smith, S. B.; Granzier, H. L.; Bustamante, C. *Science* **1997**, *276*, 1112–1116.
- (9) Li, H.; Oberhauser, A. F.; Fowler, S. B.; Clarke, J.; Fernandez, J. M. *Proc. Natl. Acad. Sci. U.S.A.* **2000**, *97*, 6527–6531.
- (10) Marszalek, P. E.; Lu, H.; Li, H.; Carrion-Vazquez, M.; Oberhauser, A. F.; Schulten, K.; Fernandez, J. M. *Nature* **1999**, *402*, 100–103.

- (11) Smith, B. L.; Schaffer, T. E.; Viani, M.; Thompson, J. B.; Frederick, N. A.; Kind, J.; Belcher, A.; Stucky, G. D.; Mors, D. E.; Hansma, P. K. *Nature* **1999**, *399*, 761–763.
- (12) Thompson, J. B.; Kindt, J. H.; Drake, B.; Hansma, H. G.; Morse, D. E.; Hansma, P. K. *Nature* **2001**, *414*, 773–776.

a. Modular multi-domain protein titin



b. Biomimetic design of modular polymer having multiple loops

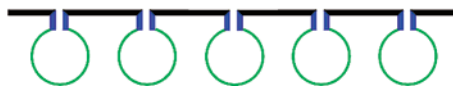


Figure 1. Concept of biomimetic modular polymer design. (a) A small section of titin, which has 200–300 repeating immunoglobulin (Ig) domains. (b) The design of modular polymer containing multiple loops held by secondary forces.

physical properties for synthetic materials. In this report, we use titin as a model to design the first synthetic polymers having well-defined modular structures by using strong hydrogen-bonding units (Figure 1). We also report our investigation of their nanomechanical properties at the single-molecule level through atomic force microscopy (AFM) and the correlation of the single-molecule properties with macroscopic material properties.

Results and Discussion

Based on molecular modeling and single-molecule studies, the six hydrogen bonds between β -strands A' and G in the immunoglobulin (Ig) module of titin play a critical role in its mechanical stability.²¹ In our biomimetic design, a strong quadruple hydrogen bonding motif, 2-ureido-4-pyrimidone (UPy), was employed to direct the formation of loops along a polymer chain. Meijer and co-workers have shown beautifully that UPy dimerizes strongly with a dimerization constant $K_{\text{dim}} > 10^8 \text{ M}^{-1}$ in toluene.²² Based on the magnitude of the dimerization constant, the free energy required to break the UPy dimer is more than 10.9 kcal/mol. This is comparable to protein unfolding energy and lower than typical covalent bond energies, and, therefore, suits our biomimetic study.

The synthesis of the UPy-containing monomers began with the alkylation of ethyl acetoacetate with allyl bromide followed by condensation with guanidine carbonate to afford an isocytosine, which was further treated with allyl isocyanate to provide compound **2** (Scheme 1a). The isocytosine ring was protected as *para*-nitrobenzyl (PNB) ether for improved solubility and also for further synthesis of a control polymer to be used in comparative studies. Hydroboration of the diolefin **3** afforded the protected UPy-containing monomer **4**. The PNB protection was removed by catalytic hydrogenation to give the free UPy monomer **5**. Both the protected UPy monomer **4** and the free UPy monomer **5** will be incorporated into polymer chains for comparative studies.

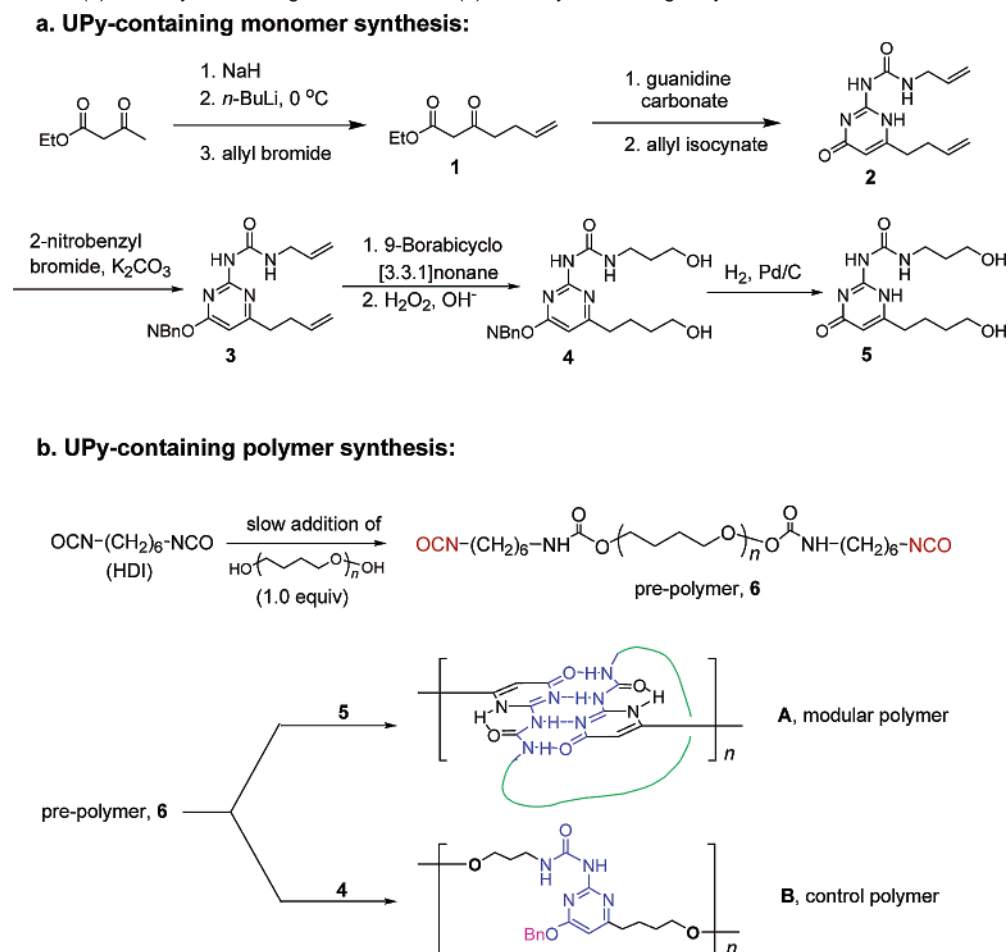
Polymerization reactions were carried out via prepolymer formation followed by chain extension. Poly(tetramethylene glycol) (PTMG, 1 equiv, with a number average molecular weight, M_n , of 1400 g/mol) was injected slowly by a syringe pump into a solution of 2 equiv of 1,6-diisocyanatohexane to form a prepolymer. The PNB-protected UPy monomer **4** was added as a chain extender to complete the polymerization process, providing a fully protected control polymer **B** that is unable to form UPy dimers because the quadruple hydrogen bonding sites are blocked by the PNB protection (Scheme 1b). Polymerization reactions with the free UPy monomer **5** were carried out in the same manner, providing a deprotected polymer **A** in which the free UPy units dimerize to form loops along polymer chains (Scheme 1b). Proton nuclear magnetic resonance spectroscopy (¹H NMR) confirmed the formation of UPy dimers in polymer **A**, showing three characteristic peaks for the hydrogen-bonding protons of the UPy dimer at 10.28, 11.95, and 13.20 ppm. For the control polymer **B**, only one intramolecularly hydrogen bonded proton was observed at 9.2 ppm. Comparison of the ¹H NMR spectrum of polymer **A** with those of other UPy dimer systems reported in the literature revealed that the UPy units exist as keto tautomers in our system.²³ The number-averaged molecular weights of the polymers are typically about 70 000 g/mol as measured by gel permeation chromatography (GPC) using polystyrene standards.

Both the control polymer (**B**) and the modular polymer having multiple loops (**A**) were subjected to single-molecule force-extension studies using AFM. The single-molecule nanomechanical properties for many biopolymers including proteins,^{7–10} polysaccharides,²⁴ DNAs,²⁵ and synthetic polymers²⁶ have been studied in aqueous environment using AFM. For our polymers, water is a poor solvent and disrupts the hydrogen bonding between the UPy dimers. Previous studies have shown that stretching a single polymer chain in its collapsed conformation (in poor solvents or in air) gave curves that are not related to the polymer secondary structure due to the Rayleigh–Plateau instability.²⁷ To obtain meaningful force spectra reflecting the inherent structure of our polymers, our single-chain stretching experiments were done in toluene, which is a good solvent for the polymer and should preserve the hydrogen bonding in the UPy dimers because of its low polarity. A special liquid-cell reservoir was custom-built for our AFM studies to accommodate the low surface tension of toluene in sealing the liquid cell.

We followed similar protocols reported previously^{7,11,26,28} in single-chain studies of our polymers using AFM. Either the modular polymer **A** or the control polymer **B** was allowed to be adsorbed from a dilute solution (10^{-5} – 10^{-7} M) onto a freshly coated gold surface. The sample was probed in our custom-built liquid cell using toluene as the solvent. Following other studies, physisorption was used to pick up a polymer chain by the AFM tip (Si_3N_4 tips; Park Scientific Instrument). When the

- (13) Hill, D. J.; Mio, M. J.; Prince, R. B.; Hughes, T. S.; Moore, J. S. *Chem. Rev.* **2001**, *101*, 3893–4011.
- (14) Cheng, R. P.; Gellman, S. H.; DeGrado, W. F. *Chem. Rev.* **2001**, *101*, 3219–3232.
- (15) Nowick, J. S. *Acc. Chem. Res.* **1999**, *32*, 287–296.
- (16) Cornelissen, J. J. L. M.; Donners, J. J. J. M.; de Gelder, R.; Graswinckel, W. S.; Metselaar, G. A.; Rowan, A. E.; Sommerdijk, N. A. J. M.; Nolte, R. J. M. *Science* **2001**, *293*, 676–680.
- (17) Hirschberg, J. H.; Brunsveld, L.; Ramzi, A.; Vekemans, J. A.; Sijbesma, R. P.; Meijer, E. W. *Nature* **2000**, *407*, 167–170.
- (18) Zimmerman, S. C.; Wendland, M. S.; Rakow, N. A.; Zharov, I.; Suslick, K. S. *Nature* **2002**, *418*, 399–403.
- (19) Lehn, J. M. *Angew. Chem.* **1988**, *100*, 91–116.
- (20) Berl, V.; Huc, I.; Khoury, R. G.; Krische, M. J.; Lehn, J.-M. *Nature* **2000**, *407*, 720–723.
- (21) Lu, H.; Schulten, K. *Biophys. J.* **2000**, *79*, 51–65.
- (22) Sijbesma, R. P.; Beijer, F. H.; Brunsveld, L.; Folmer, B. J. B.; Hirschberg, J. H. K. K.; Lange, R. F. M.; Lowe, J. K. L.; Meijer, E. W. *Science* **1997**, *278*, 1601–1604.

- (23) Beijer, F. H.; Sijbesma, R. P.; Kooijman, H.; Spek, A. L.; Meijer, E. W. *J. Am. Chem. Soc.* **1998**, *120*, 6761–6769.
- (24) Rief, M.; Oesterhelt, F.; Heymann, B.; Gaub, H. E. *Science* **1997**, *275*, 1295–1297.
- (25) Smith, S. B.; Cui, Y.; Bustamante, C. *Science* **1996**, *271*, 795–799.
- (26) Ortiz, C.; Hadziioannou, G. *Macromolecules* **1999**, *32*, 780–787.
- (27) Haupt, B. J.; Senden, T. J.; Sevick, E. M. *Langmuir* **2002**, *18*, 2174–2182.
- (28) Li, H.; Linke, W. A.; Oberhauser, A. F.; Carrion-Vazquez, M.; Kerkvliet, J. G.; Lu, H.; Marszalek, P. E.; Fernandez, J. M. *Nature* **2002**, *418*, 998–1002.

Scheme 1. Synthesis of (a) the UPy-Containing Monomers and (b) the UPy-Containing Polymers^a

^a In modular polymer **A**, the green loop stands for the PTMG linker.

tip was retracted, extension curves such as the ones shown in Figure 2 were recorded.

The single-chain force–extension curves for both the control polymer (**B**) and the modular polymer (**A**) are shown in Figure 2. For the control polymer **B** that does not have the modular structure, we typically only observed a single peak²⁹ that is characteristic for entropic extension of a random coil chain (Figure 2b). On the contrary, the modular polymer **A** consistently showed distinct sawtooth patterns in the force–extension curve (Figure 2a and c),³⁰ similar to those observed in titin and other modular biopolymers.^{7–10} The big contrast for the force–extension curves observed for the polymers **A** and **B** strongly suggests the sequential unfolding of the UPy dimers along the modular polymer **A** chain. As the polymer chain was stretched, the force rose gradually until one UPy dimer could not sustain the force and broke instantaneously, adding additional length

to the polymer chain. Therefore, the peak force corresponds to the force required to break a UPy dimer at a specific pulling rate, and the spacing between the peaks represents the gain in length during the unfolding.³¹

Further evidence for the single-chain stretching comes from fitting the force–extension data with the wormlike chain (WLC) model (eq 1), which predicts the relationship between the extension of a single polymer chain (x) and the entropic restoring force generated ($F(x)$).^{7,32} The adjustable parameters of the WLC model are the persistence length, b , and the contour length of the polymer, L . The k and T in eq 1 are the Boltzmann constant and temperature, respectively.

$$F(x) = (kT/b)[0.25(1 - x/L)^{-2} - 0.25 + x/L] \quad (1)$$

Both the control polymer (**B**) and the modular polymer (**A**) could be fit nicely with the WLC model with a persistence length of 0.2 nm (Figure 2b and c, solid lines). Persistence lengths ranging

(29) In pulling the protected UPy control polymer **B**, we most time observed only a single peak. At about 0.1% rate, we observed two or more peaks on one curve. For those showing multiple peaks, they could not be fitted with the wormlike chain (WLC) model for a single chain, indicating that the multiple peaks originated from multiple chain adsorptions.

(30) In pulling the deprotected UPy modular polymer **A**, the success rate of picking up a chain is about 2%. In one set of experiments with a total of 48 force–extension curves, the statistical information is as follows: 6 curves show two peaks, 16 curves show three peaks, 16 curves show four peaks, 7 curves show five peaks, 2 curves show six peaks, and 1 curve shows seven peaks. Among all the unfolding peaks observed from this pool of curves, 52 peaks show peak force around 100 pN and 61 peaks show peak force around 200 pN. Of this pool of curves, about 70% of the final extension is in the range of 200–300 nm.

(31) Whereas the single-molecule stretching data could be explained by other alternative mechanisms, we believe our current explanation is the simplest and most straightforward one to account for the experimental data. The difficulty here is that there is no definitive way to rule out any other possibility. The adsorption was done in very dilute polymer solution to avoid aggregation. Before collecting the force–extension data, the AFM tip was gradually pulled away from the surface step by step to get rid of weak nonspecific interactions and finally leave one single chain strongly adsorbed on the substrate and AFM tip. We did pick up multiple chains from time to time, but in those cases, the multiple peaks could not be fitted with the WLC single-chain model.

(32) Bustamante, C. *Science* **1994**, *265*, 1599–1600.

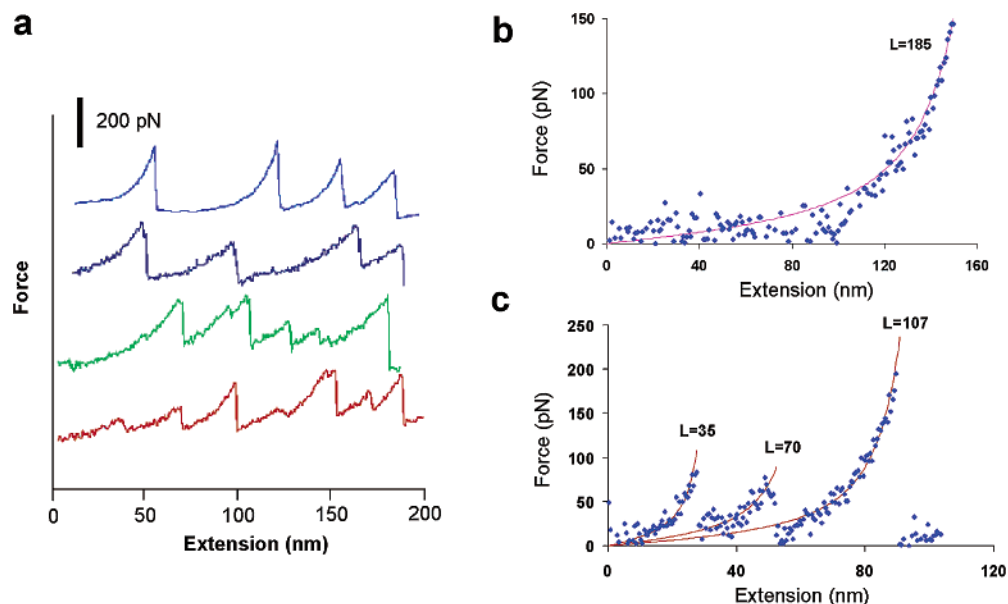


Figure 2. AFM single chain force–extension data. Both the modular polymer **A** and the control polymer **B** were subjected to single-chain force–extension studies in toluene. Whereas a single stretching peak was usually observed for the control polymer **B**, the characteristic sawtooth pattern was observed for the modular polymer **A**. In Figure 2b and c, all scattered dots represent experimental data and the solid lines are results from WLC fitting. (a) An overlay of representative force–extension curves for modular polymer **A**. Sawtooth patterned curves were consistently obtained.³⁰ (b) One representative single-chain force–extension curve for the control polymer **B**, in which only one peak was observed. (c) A single-chain force–extension curve for the modular polymer **A** shows the characteristic sawtooth pattern with three peaks.

from 0.22 to 0.4 have been reported for various synthetic polymers and natural proteins based on WLC fitting of single-chain stretching data.^{26,33,34} These values are typically lower than those obtained from classical bulk scattering measurements.³⁵ This discrepancy in persistence length is generally accounted for by the limitation of the WLC model;³⁶ nevertheless, this model has been successfully applied to fit force–extension data for many natural and synthetic polymer systems. For our polymers **A** and **B**, the major chemical composition of the main chains is the flexible polyether (PTMG). A persistence length of 0.2 nm is reasonable for our system when compared with the 0.4 nm values for titin and other proteins, which should have larger persistence lengths because of their more rigid polypeptide backbones.

Biological modular polymers such as titin show a constant increase in contour length (ΔL) between consecutive peaks in their force–extension curves due to the sequential unfolding of identical modules as the polymer is stretched. In contrast, the gain in contour length upon opening of each loop is not constant for our modular polymer **A** (Figure 2a and c). The nonconstant ΔL values are attributed to three factors for the modular polymer **A**: (1) polydispersity of the PTMG linker (PDI ≈ 2.2 by GPC), (2) partial chain extension during prepolymer formation, and (3) possible random dimerization of UPy units on polymer chains. In addition to the polydisperse nature of the PTMG, during the prepolymer formation in the first step of polymerization, partial chain extension may occur to elongate the loop length. Furthermore, one UPy unit may dimerize with another nonadjacent UPy unit on the chain, which will randomize the loop size. Similar kinds of “misfolding” have been

observed in biological modular polymers.³⁷ Even though the ΔL values are not constant, the consistent stepwise increase in contour length suggests the sequential unfolding of UPy modules along the polymer **A** chain as it was stretched.

A more subtle observation was that two peak forces were consistently observed in the force spectra of the polymer **A** (Figure 2a), one at a lower force of ~ 100 pN and another at a higher force of ~ 200 pN.³⁰ We propose this is due to different UPy dimer topologies formed along polymer chains. During polymerization to form the modular polymer **A**, the UPy units can be connected by the diisocyanate prepolymer in head-to-head, head-to-tail, or tail-to-tail fashions. These different connectivities will lead to the formation of the following three different UPy dimer topologies, **I–III** (Scheme 2): The unfolding of dimers **I** and **II** should require a stronger force than the unfolding of dimer **III** because, for both **I** and **II**, the quadruple hydrogen bonds need to be broken cooperatively, whereas, for **III**, the module can be “peeled off” gradually. We propose that the higher force peaks are attributed to the unfolding of types **I** and **II** UPy dimers and the lower force peaks are attributed to the unfolding of type **III** UPy dimer.

The mechanical properties of the polymers were tested in bulk as well to correlate with the single-chain nanomechanical studies. Polymer samples were cast into thin films and subjected to stress–strain analyses using Mini-Instron. Figure 3 shows the comparison of stress–strain data for the modular polymer **A**, the control polymer **B**, and a regular polyurethane (PU, $M_n \sim 1000,000$ g/mol) that does not contain any UPy units. On a stress–strain curve, the maximum stress at break gives the tensile strength of the material, while the whole area covered under the curve reflects the total energy required to break the material, that is, the toughness. The introduction of protected UPy units into the polyurethane enhanced its tensile strength

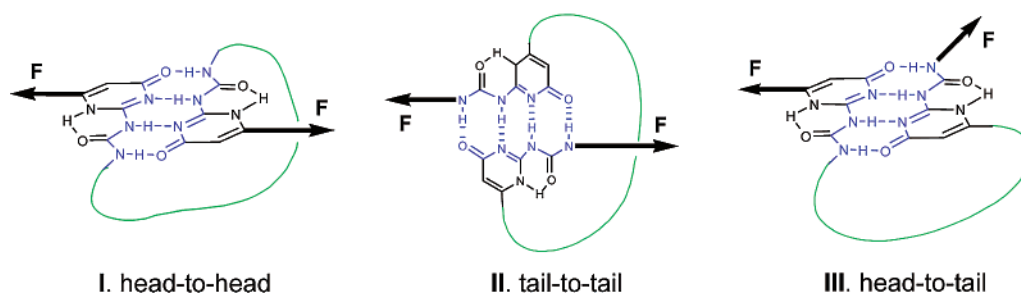
(33) Bemis, J. E.; Akhremitchev, B. B.; Walker, G. C. *Langmuir* **1999**, *15*, 2799–2805.

(34) Senden, T. J.; di Meglio, J.-M.; Auroy, P. *Eur. Phys. J. B* **1998**, *3*.

(35) Flory, P. J. *Principles of Polymer Chemistry*; 1953.

(36) Rief, M.; Pascual, J.; Saraste, M.; Gaub, H. E. *J. Mol. Biol.* **1999**, *286*, 553–561.

(37) Oberhauser, A. F.; Marszalek, P. E.; Carrion-Vazquez, M.; Fernandez, J. M. *Nat. Struct. Biol.* **1999**, *6*, 1025–1028.

Scheme 2. Three Possible Topologies for UPy Dimers I–III^a

^a The flexible loops in green color in the drawings are the PTMG linkers. The arrows represent the directions of forces applied to the UPy dimer modules.

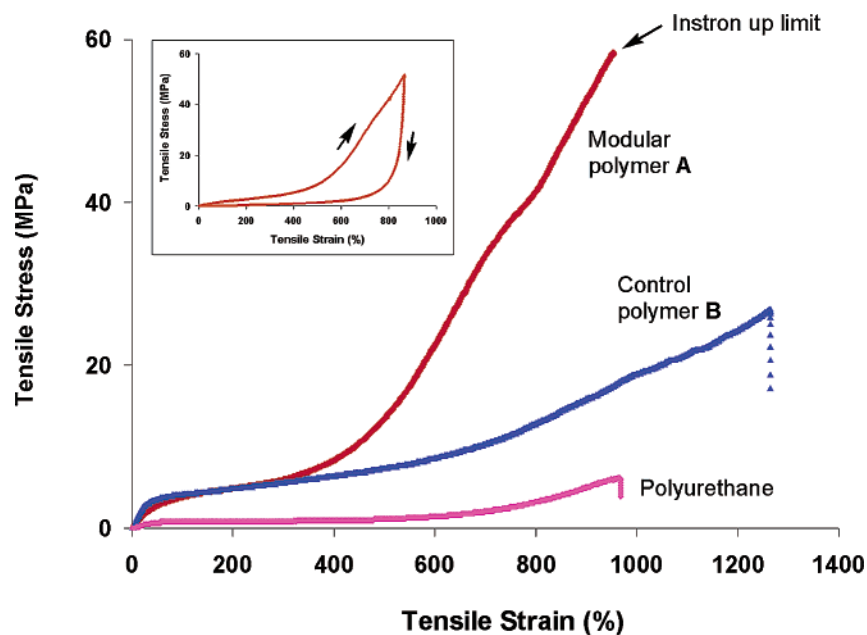


Figure 3. Stress–strain curves for the control and modular polymers. The curve in the bottom (magenta) is for the polyurethane (PU) made from PTMG and HDI without any UPy units. The curve in the middle (blue) is the control polymer **B** containing the protected UPy units. The curve at the top (red) is for the modular polymer **A** containing UPy dimerized loops. The modular polymer **A** could not be broken by the Mini-Instron at its maximum load. A stretching–retraction cycle for the polymer **A** is shown in the inset, which shows a huge hysteresis, indicating great energy dissipation during the cycle.

and toughness. Even though the PNB protection blocked the UPy from dimerization to form loops, π – π stacking, dipole–dipole interactions, and weak residual hydrogen bonding between the protected UPy units should increase the tensile strength and toughness of the protected polymer **B**. For polymer **A**, in which UPy units can dimerize to form loops along the chains, the stress–strain curve shows dramatic differences from the curve of the control polymer (**B**). It shows a sigmoid stress–strain curve characteristic for elastic polymers. After a pseudo yield region, the sample becomes much stiffer with a significant increase in modulus and strength. Due to its high strength and toughness, the ultimate tensile strength at break and the fracture toughness could not be obtained for polymer **A** because the sample could not be broken even at the maximum load of the Mini-Instron for the smallest sample specimen we could prepare. Nevertheless, quantitative comparisons can be made at 950% strain for the three samples. At 950% strain, the tensile stresses are 58.2, 17.4, and 6.0 MPa, and the energy absorptions per unit volume are 191.5, 78.5, and 17.7 MPa, respectively, for the modular polymer **A**, the control polymer **B**, and the PU samples. This comparison clearly shows that the modular polymer **A** is significantly stronger and tougher than either the control polymer **B** or the simple PU. The polymer **A** is also very elastomeric, as evidenced by the high strain up to 900%

and the complete recovery to its original length in three consecutive extension–retraction experiments. The huge hysteresis accompanied in one extension–retraction cycle (inset in Figure 3) further reveals the great energy dissipation capability of the system, an important feature for high toughness. The bulk mechanical data correlate well with our single-chain force–extension observation, which successfully demonstrates our biomimetic concept: the introduction of modular structures held by sacrificial weak bonds into a polymer chain can successfully combine the three most fundamental mechanical properties, i.e., high tensile strength, toughness, and elasticity, into one polymer.

Classical polymer theory has predicted that many physical properties of bulk polymers can be explained in terms of the behavior of single molecules.^{1,35} For very large macromolecules, contributions from inter- and intramolecular interactions to bulk physical properties become difficult to distinguish, and molecular and macroscopic mechanical properties merge.¹ In bulk films, the UPy units may dimerize within the same chain to form intramolecular loops or dimerize between chains to form intermolecular loops. From a macroscopic property point of view, both breaking intramolecular loops and breaking intermolecular UPy dimers require force and absorb energy. As has been discussed previously for the adhesive biopolymers in

biominerals such as seashell and bone,^{11,12} both the successive opening of intrachain loops or folded domains within a single molecule and the successive release of sacrificial interchain bonds should contribute to the extremely high toughness of these materials. In our modular polymer **A**, the unfolding of both intramolecular and intermolecular loops should contribute to the significantly enhanced mechanical properties, i.e., the combination of high tensile strength, fracture toughness, and elasticity.

Conclusion

A novel biomimetic modular polymer design is reported here to address the challenge of designing synthetic polymers with a combination of mechanical strength, toughness, and elasticity. Following the molecular mechanism used in the skeletal muscle protein titin, modular polymers containing multiple loops were constructed by using precise and strong hydrogen-bonding units. Single-molecule force–extension studies were conducted for both the control polymer and the polymer containing many folded loops, which revealed the sequential unfolding of loops as a modular polymer chain is stretched. Bulk stress–strain experiments demonstrated that the modular polymer containing many loops successfully combine high mechanical strength, toughness, and elasticity. The excellent correlation between the single-molecule and the bulk properties successfully demonstrates our biomimetic concept of using a modular domain structure for advanced polymer properties. We are currently developing modular polymers containing new better-defined nanodomain structures. The molecular parameters of the nanodomains will be varied to systematically investigate the relationship between molecular structures and the single-molecule mechanical properties, which will be correlated with the nanoscopic and macroscopic mechanical properties of the materials. Insight into the relationship between the molecular properties of polymeric materials and their macroscopic performance should allow us to begin to develop rational materials designs: working up from molecular design to select desired materials characteristics to perform in particular applications.

Experimental Section

I. Synthesis and Characterization of Monomers and Polymers.

General. ¹H NMR spectra were recorded at 400 and 500 MHz, and ¹³C NMR spectra were recorded at 125 and 100 MHz on Bruker instruments. ¹H and ¹³C NMR chemical shifts are reported as δ values in ppm relative to TMS or residual solvent. Mass spectral data was obtained on a Micromass autospec spectrometer. Combustion analyses were performed by Atlantic Microlab (Norcross, GA). Gel permeation chromatography (GPC) was carried out using an Agilent 1100 Series GPC-SEC Analysis System along with a mixed bed Plgel Mixed-C column from Polymer Labs. The eluent was CHCl₃/DMF (95:5), and a flow rate of 0.500 mL/min was used. The calibration was performed using polystyrenes from Aldrich as standards. All commercial reagents were used as received with the following exceptions: the solvents CH₂-Cl₂, THF, and toluene were obtained from an alumina filtration system. Liquid chromatography was performed using forced flow (flash chromatography) of the indicated solvent system on Fisher silica gel 60 (230–400 mesh). Moisture sensitive reactions were carried out under a nitrogen atmosphere using flame-dried glassware and standard syringe/septa techniques.

3-Oxo-hept-6-enoic Acid Ethyl Ester (1). THF (100 mL) was added to a flask charged with NaH (3.23 g, 134 mmol). The resulting suspension was cooled to 0 °C and ethyl acetoacetate (12.0 mL, 94.0 mmol) was added via syringe pump over 1 h. The clear solution was

cooled to –78 °C, and 2.5 M *n*-butyllithium (45.0 mL, 113 mmol) was added dropwise via syringe pump over 1 h. The reaction was allowed to warm to room temperature and stir overnight. The yellow solution was quenched with DI H₂O (300 mL) and extracted with ether (3 × 200 mL). The combined extracts were dried over MgSO₄, concentrated *in vacuo*, and purified by flash chromatography (silica, 4% acetone/hexanes) to give **1** as a colorless oil (10.22 g, 57%). ¹H NMR (500 MHz, CDCl₃) δ 1.29 (t, *J* = 7.1 Hz, 3H), 2.36 (m, 2H), 2.65 (t, *J* = 7.2 Hz, 2H), 3.45 (s, 2H), 4.21 (q, *J* = 7.1 Hz, 2H), 5.02 (m, 2H), 5.81 (m, 1H); ¹³C NMR (125 MHz, CDCl₃) δ 14.68, 27.82, 42.45, 49.78, 61.79, 115.97, 137.19, 167.57, 180.93, 202.41. HRMS *m/z*: (NH₃ – Cl) calcd for C₉H₁₄O₃, 170.0943; found, 170.0944.

2-Amino-6-but-3-enyl-1H-pyrimidin-4-one. Guanidine carbonate (5.41 g, 30.0 mmol) was added to a solution of **1** (10.22 g, 60.06 mmol) and ethanol (500 mL). The reaction was heated to reflux for 14 h and then cooled to room temperature.³⁸ The ethanol was removed *in vacuo*, and the resulting solid was collected by vacuum filtration to give 2-amino-6-but-3-enyl-1H-pyrimidin-4-one as white crystals (4.2 g, 43%). ¹H NMR (500 MHz, DMSO) δ 2.28 (m, 2H), 4.96 (d, *J* = 12.2 Hz, 1H), 5.03 (d, *J* = 17.3 Hz, 1H), 5.38 (s, 1H), 5.81 (m, 1H), 6.47 (s, 2H), 10.65 (s, 1H); ¹³C NMR (125 MHz, CDCl₃) δ 31.54, 35.95, 99.88, 100.31, 115.15, 137.84, 155.71, 163.97. HRMS *m/z*: (NH₃ – Cl) calcd for C₈H₁₁N₃O, 165.0902; found, 165.0907.

1-Allyl-3-(6-but-3-enyl-4-oxo-1,4-dihydro-pyrimidin-2-yl)-urea (2). Allyl isocyanate (3.15 mL, 35.6 mmol) was added to a solution of 2-amino-6-but-3-enyl-1H-pyrimidin-4-one (4.20 g, 23.4 mmol) and pyridine (75 mL). The reaction was heated to reflux for 4 h.³⁸ After cooling to room temperature, the pyridine was removed *in vacuo* by codistillation with toluene. The crude solid was recrystallized from a minimum amount of ethanol to give **2** as white crystals (4.84 g, 77%). ¹H NMR (500 MHz, CDCl₃) δ 2.41 (m, 2H), 2.57 (m, 2H), 3.90 (m, 2H), 5.17 (m, 1H), 5.29 (d, *J* = 18.8 Hz, 1H), 10.43 (s, 1H), 12.00 (s, 1H), 13.14 (s, 1H); ¹³C NMR (125 MHz, CDCl₃) δ 31.25, 32.41, 42.65, 106.69, 116.31, 117.47, 134.68, 135.57, 151.98, 155.09, 157.10, 173.52. HRMS *m/z*: (NH₃ – Cl) calcd for C₁₂H₁₆N₄O₂, 248.1273; found, 248.1270.

1-Allyl-3-[4-but-3-enyl-6-(2-nitrobenzyloxy)pyrimidin-2-yl]-urea (3). 2-Nitrobenzyl bromide (6.94 g, 32.1 mmol) was added to a mixture of **2** (3.99 g, 16.1 mmol), potassium carbonate (4.44 g, 32.1 mmol), and DMF (70 mL). The reaction was heated to 70 °C for 24 h.^{38–40} After cooling to room temperature, the inorganic salts were removed by vacuum filtration. DMF was removed *in vacuo* by codistillation with toluene. The resulting brown oil was diluted with DI H₂O (250 mL) and extracted with CHCl₃ (5 × 150 mL). The organic extracts were combined, dried over MgSO₄ and concentrated *in vacuo* to an orange solid. Tritration in hot ether gave **3** as a white solid (5.56 g, 90%). ¹H NMR (500 MHz, CDCl₃) δ 2.44 (m, 2H), 2.72 (m, 2H), 4.00 (t, *J* = 4.5 Hz, 2H), 5.13 (m, 2H), 5.14 (d, *J* = 10.3 Hz, 1H), 5.26 (d, *J* = 17.1 Hz, 1H), 5.75 (s, 2H), 5.85 (m, 1H), 5.93 (m, 1H), 6.29 (s, 1H), 7.51 (m, 1H), 7.65 (m, 2H), 8.13 (d, *J* = 8.2 Hz, 1H), 9.26 (s, 1H); ¹³C NMR (125 MHz, CDCl₃) δ 32.39, 36.92, 42.74, 65.26, 100.42, 115.94, 116.23, 125.49, 129.21, 129.49, 132.78, 134.15, 135.11, 137.22, 154.43, 157.76, 170.09. HRMS *m/z*: (NH₃ – Cl) calcd for C₁₉H₂₁N₅O₄, 383.1594; found, 383.1598.

1-[4-(4-Hydroxybutyl)-6-(2-nitrobenzyloxy)pyrimidin-2-yl]-3-(3-hydroxypropyl)-urea (4). A solution of **3** (5.30 g, 13.8 mmol in 20 mL of THF) was added to a flask charged with a 0.5 M solution of 9-borabicyclo[3.3.1]nonane (9-BBN) (74.7 mL, 37.3 mmol). The reaction stirred at room temperature for 2 h. Ethanol (22.4 mL), 6 N NaOH (7.5 mL), and 30% H₂O₂ (15.0 mL) were added sequentially. The reaction was heated to 50 °C for 2 h.⁴¹ After cooling to room temperature, a saturated solution of potassium carbonate was added

(38) Ky Hirschberg, J. H. K.; Beijer, F. H.; van Aert, H. A.; Magusin, P. C. M. M.; Sijbesma, R. P.; Meijer, E. W. *Macromolecules* **1999**, *32*, 2696–2705.

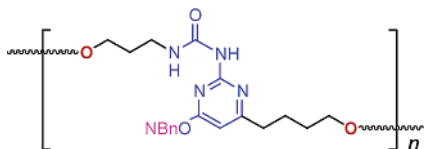
(39) Bochet, C. G. J. *Chem. Soc., Perkin Trans. 1* **2002**, 125.

(40) Zehavi, U.; Amit, B.; Patchornik, A. *J. Org. Chem.* **1972**, *37*, 2281–2285.

(50 mL). The organic layer was separated, dried over potassium carbonate, and concentrated in vacuo to brown oil. Purification by flash chromatography (silica, CHCl_3 to 5% $\text{MeOH}/\text{CHCl}_3$) gave a slightly yellow solid which was recrystallized from a minimum amount of acetone to give **4** as white crystals (5.79 g, 54%). $^1\text{H NMR}$ (500 MHz, DMSO) δ 1.43 (m, 2H), 1.63 (m, 4H), 2.60 (t, $J = 7.5$ Hz, 2H), 3.26 (m, 2H), 3.41 (m, 2H), 3.47 (m, 2H), 4.42 (t, $J = 5.1$ Hz, 1H), 4.51 (t, $J = 5.1$ Hz, 1H), 5.72 (s, 2H), 6.44 (s, 1H), 7.64 (m, 1H), 7.77 (m, 2H), 8.13 (d, $J = 7.9$ Hz, 1H), 9.19 (t, $J = 5.4$ Hz, 1H), 9.48 (s, 1H); $^{13}\text{C NMR}$ (125 MHz, DMSO) δ 24.30, 31.896, 32.54, 36.15, 36.41, 58.48, 60.40, 64.21, 98.91, 124.89, 129.33, 129.78, 131.80, 134.14, 147.48, 153.97, 157.64, 169.12, 171.15. HRMS m/z : ($\text{NH}_3 - \text{Cl}$) calcd for $\text{C}_{19}\text{H}_{26}\text{N}_5\text{O}_6$, 420.1883; found, 420.1876.

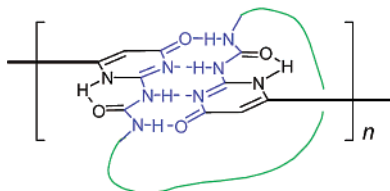
1-[6-(4-Hydroxybutyl)-4-oxo-1,4-dihydropyrimidin-2-yl]-3-(3-hydroxypropyl)-urea (5). Palladium on carbon (10 wt. percent, 5.3 mg) was added to a solution of **4** (341 mg, 1.20 mmol) in methanol (10 mL). The solution was stirred under an atmosphere of hydrogen for 12 h. Nitrogen was bubbled through the solution of 12 h, and the palladium was removed by filtration through Celite. The solution was concentrated in vacuo to a pink solid. Tritration with acetone followed by recrystallization from *n*-butanol gave pure **5** (284 g, 83%) as a white solid. $^1\text{H NMR}$ (500 MHz, DMSO) δ 1.42 (m, 2H), 1.60 (m, 4H), 2.36 (t, $J = 7.4$, 2H), 3.20 (q, $J = 6.4$, 2H), 3.40 (q, $J = 6.4$, 2H), 3.45 (q, $J = 5.2$, 2H), 4.38 (t, $J = 5.1$, 1H), 4.52 (t, $J = 5.0$, 1H), 5.75 (s, 1H), 7.45 (s, 1H), 9.71 (s, 1H), 11.49 (s, 1H); $^{13}\text{C NMR}$ (125 MHz, DMSO) δ 24.39, 32.34, 32.76, 36.58, 36.89, 58.83, 60.84, 104.41, 152.76, 155.93, 163.38, 168.15. HRMS m/z : ($\text{NH}_3 - \text{Cl}$) calcd for $\text{C}_{12}\text{H}_{20}\text{N}_4\text{O}_4$: 284.1485; found, 284.1485.

Polymerization with Protected UPy-Containing Monomers to Make the Control Polymer (B). PTMO ($M_n = 1400$ g/mol) (0.70 mL, 0.50 mmol) was added dropwise to a solution of 1,6-diisocyanatohexane (168 μL , 1.00 mmol) and DMAc (0.50 mL). The solution stirred at room temperature for 60 min, then a solution of **5** (209 mg, 0.500 mmol) in DMAc (0.50 mL) was added dropwise. The solution stirred at room temperature for 18 h, resulting in a very viscous solution. Precipitation from methanol (200 mL) provided polymer **B** as a white elastomer.



GPC using CHCl_3/DMF (95:5) as the eluent measured the average molecular weights as $M_n = 69\,000$ g/mol, $M_w = 115\,000$ g/mol; $M_w/M_n = 1.66$, $T_g = 0.61$ °C. $^1\text{H NMR}$ (500 MHz, CDCl_3) δ 1.25, 1.32, 1.48, 1.61, 1.92, 2.65, 2.14, 3.41, 4.06–4.20, 4.62–5.38, 5.72, 6.28, 7.49, 7.67, 8.12, 9.25.

Polymerization with Deprotected UPy-Containing Monomers to Make the Modular Polymer (A). PTMO ($M_n = 1400$ g/mol) (0.70 mL, 0.50 mmol) was added dropwise to a solution of 1,6-diisocyanatohexane (168 μL , 1.00 mmol) and DMAc (0.50 mL). The solution stirred at room temperature for 60 min, and then a solution of **6** (142 mg, 0.500 mmol) in DMAc (0.50 mL) was added dropwise. The solution stirred at room temperature for 18 h, resulting in a very viscous solution. Precipitation from methanol (200 mL) provided polymer **A** as a colorless elastomer.



GPC using CHCl_3/DMF (95:5) as the eluent measured the average molecular weights as $M_n = 68\,000$ g/mol, $M_w = 123\,000$ g/mol; $M_w/M_n = 1.80$, $T_g = 6.92$ °C. $^1\text{H NMR}$ (500 MHz, CDCl_3) δ 1.25, 1.32, 1.48, 1.61, 1.92, 2.52, 3.15, 3.41, 4.06–4.11, 4.40–5.36, 5.82, 10.2, 11.8, 13.1.

II. Single-Chain Force–Extension Measurements by Atomic Force Microscopy. Preparation of Physically Adsorbed Polymers onto Au-Coated Silicon Wafers. Polymers **A** and **B** were adsorbed onto freshly gold coated silicon wafers (1.2 cm \times 1.2 cm) by immersion in a solution of polymer (0.2 mg/mL) in $\text{CHCl}_3/\text{DMAc}$ (95:5) for 8 h. The sample was removed from the solution and sonicated (3 \times 5 min) in CHCl_3 . Samples were dried under a stream of nitrogen and used immediately.

Atomic Force Microscopy Force–Extension Experiments. A CP Research atomic force microscope equipped with a 100 μm scanner from Park Scientific Instruments was used to carry out the AFM single-chain stretching experiments. ProScan software (version 1.6) was used for all of the data acquisition. Force–extension experiments were carried out in toluene (filtered by 0.02 μm membrane). The prepared sample was loaded into a custom-built liquid reservoir filled with filtered toluene at room temperature. A micro-liquid-cell (purchased from Park Scientific Instruments) equipped with silicon nitride cantilevers (microlevers, purchased from www.store.veeco.com) was allowed to approach the surface. We used the microlever C, which has a force constant in the range of 14.4 to 15.7 pN/nm as calibrated by the Asylum Research, to collect the force–extension data. Force versus distance curves were acquired using a spectroscopy mode (ML06C cantilever) with a frequency of 0.3–0.5 Hz and a distance of 0.2–0.7 μm , correlating to pulling speeds of 0.06–0.35 $\mu\text{m/s}$.

III. Stress–Strain Analysis using Instron. Silanization of Glass Petri Dishes for Film Casting. Glass Petri dishes were cleaned with a freshly prepared mixture of concentrated sulfuric acid and 30% hydrogen peroxide (70:30, v:v) at 120 °C for 30 min. The dishes were removed and washed with a large amount of DI water and rinsed with acetone.⁴² The dishes were blown dry under a stream of nitrogen and immediately used in the silanization procedures. The formation of the trimethylsilyl layer on the glass Petri dishes was carried out in the vapor phase under reduced pressure. The cleaned substrates and a small vial (Fisher brand 12 \times 35 mm², 0.5 DR) containing 150 μL of trimethylsilyl chloride were placed inside a vacuum desiccator (Wheaton dry-seal desiccator, 100 mm). The desiccator was slowly evacuated using the house vacuum, sealed tightly, and kept in this condition for 16 h at room temperature.³⁹ After completion of silanization, the Petri dishes were removed, ultrasonicated in fresh acetone (5 \times 5 min), dried under a stream of nitrogen, and stored under nitrogen for future use.

Film Casting for Protected Polymer (B). Protected polymer **B** (1.41 g) was dissolved in chloroform (20 mL). The viscous solution was ultrasonicated to remove any bubbles from the solution and then poured into a TMS-treated glass Petri dish. The solvent was allowed to slowly evaporate over 12 h, and the resulting film was dried at 60 °C in a vacuum oven for 2 days. After drying, the film was stored under nitrogen for future use.

Film Casting for Deprotected Polymer (A). Deprotected polymer **A** (1.41 g) was dissolved in a mixture of chloroform and methanol (20 mL, 40:1 $\text{CHCl}_3/\text{MeOH}$). The viscous solution was ultrasonicated to remove any bubbles from the solution and then poured into a TMS-treated glass Petri dish. The solvent was allowed to slowly evaporate over 12 h, and the resulting film was dried at 60 °C in a vacuum oven for 2 days. After drying, the film was stored under nitrogen for future use.

Stress–Strain Acquisition Using Instron. An Instron Universal Testing Machine (model 5564) at Professor David Tirrell's group at

(41) Brown, H. C.; Knights, E. F.; Scouten, C. G. *J. Am. Chem. Soc.* **1974**, *96*, 7765.

(42) Moon, J. H.; Shin, J. W.; Kim, S. Y.; Park, J. W. *Langmuir* **1996**, *12*, 4621.

Caltech was used to perform stress–strain testing. A uniform strain rate of 100% gauge length per minute was chosen otherwise specified. Samples were wrapped around by same material in the region of the grips to prevent slip off or break at end. All experiments were performed at room temperature.

Acknowledgment. We are grateful for the financial support from the National Science Foundation (CAREER Award to Z.G., DMR-0135233), the Arnold and Mabel Beckman Founda-

tion (BYI Award to Z.G.), and the University of California at Irvine. We thank Professor D. A. Tirrell and P. Nowatzki at Caltech for their generous help on Mini-Instron tests, Professor M. L. Mecartney and L. Ramirez at UCI for their help on Instron tests, Professors H. G. Hansma and P. K. Hansma at UCSB for consultation on AFM studies, and Professor D. A. Brant at UCI for helpful discussions and insightful comments on the manuscript.

JA039127P